ORIGINAL ARTICLE

Electrical resistivity tomography (ERT) based subsurface characterisation of Pakhi Landslide, Garhwal Himalayas, India

Philips Omowumi Falae[1,2] · Debi Prasanna Kanungo[1] · Pradeep Kumar Singh Chauhan[1] · Rajesh Kumar Dash[1,2]

Abstract

Pakhi landslide is one of the major debris slides of retrogressive nature along national highway (NH-58) corridor from Rishikesh to Badrinath in Garhwal Himalayas, India. The present work is the first such attempt in one of the landslides in Indian Himalayas and in the present case study, the subsurface characterization of the landslide was carried out with an aim to correlate the subsurface lithology, slip surface and geometry of the landslide using borehole investigation and electrical resistivity tomography (ERT) techniques. The results from ERT survey along and across the landslide could help to delineate different strata layers; thereby deciphering the probable slip surface of the landslide activity. Further, based on the landslide model drawn from the ERT interpretations, it can be stated that the crown portion of the right flank is more vulnerable to sliding phenomenon and that of the left flank is more prone to erosion. The results obtained from both the borehole investigation and ERT techniques are observed to be in great agreement and could complement each other for subsurface detailed investigation of landslide. The integration of both these techniques provides useful information about the landslide activities and defines the geometry of the landslide. Hence, it will be quite helpful in planning mitigation strategies as well as usefulness of each of these techniques.

Keywords Landslide · ERT · Borehole · Subsurface investigation

Introduction

Landside is known as downward movement of a slope caused by various geomorphological, geological, hydrological and seismological factors under the influence of gravity (Cruden 1991). These mass movements range from very slow slides in soils to rock avalanches (Jongmans and Garambois 2007). Landslide is one of the major problems in the Himalayas due to natural processes, increase in the population of the hilly regions and quest for infrastructural development and urbanisation (van Westen et al. 2013). About 15% of India (~ 0.49 million km^2) including the mountainous areas of the Himalayas, the Meghalaya plateau and the Western Ghats are landslide-prone (NDMA 2009). Various types of landslides have been recorded within this region such as rock fall, rock toppling, rock slide, debris slide and debris flow. When landslide occurs, it is usually disastrous and sometimes leading to loss of human lives and properties. To mitigate such a hazard effectively, it is essential to develop a proper understanding of the mechanisms involved in a landslide phenomenon. Landslide occurrences are often associated with reactivation of old landslides and road cut slopes and these are characterised by high complexity and variability in space and time (de Bari et al. 2011). The complexity of landslide assessment requires integrated approach to unveil both its surface (Malet et al. 2002; Travelletti and Malet 2012) and subsurface (Grandjeans et al. 2007; Lissak et al. 2014; Fressard et al. 2016; Sastry and Mondal 2013) characteristics. Hence, the need for application of multidisciplinary methods such as satellite imagery, landslide inventory, geological/geomorphological, geophysical and geotechnical borehole investigation approaches become necessary. The integration of different techniques allows to obtain useful information for all the phases of the landslide disaster cycle, overcoming the limitations of each single method applied (Perrone et al. 2014; Strelec et al. 2017).

✉ Debi Prasanna Kanungo
  debi.kanungo@gmail.com

1 Geotechnical Engineering Group, CSIR-Central Building Research Institute (CBRI), Roorkee, Uttarakhand 247667, India

2 Academy of Scientific and Innovative Research (AcSIR), Ghaziabad, India

Before planning for detailed landslide remedial measures, any specific landslide needs to be investigated in detail in terms of topographical, geological, geophysical and geotechnical characterization of the unstable landslide area. The topographical characterization of site-specific landslide can be performed using remote sensing techniques and surveying techniques to prepare elevation contour maps on large scale. The geological mapping of the landslide is generally carried out through surface feature mapping of different types of materials on the hill slope including soil/debris and rock strata. Geotechnical investigation in landslide area involves borehole drilling as the direct way of subsurface characterization and collection of landslide material over different depths for laboratory testing and analysis. Borehole drilling is cost- and labour-intensive and also gives subsurface information of a particular location in the landslide area. To fill up the subsurface information gaps between the boreholes, geophysical investigations and interpretation of geophysical data are better alternatives to obtain useful information about the subsurface material in the landslide area and also the probable slip surface (Rezaei et al. 2018; Bellanova et al. 2018). Geophysical investigation techniques have been widely and successfully employed for many years for various problematic engineering sites associated with exploration of natural resources, engineering geological, geotechnical and environmental concerns (Giocoli et al. 2015). In recent times, geophysical techniques in conjunction with other geotechnical investigation techniques are becoming more and more popular in different parts of the globe for landslide investigations in terms of material thickness across depths (Reci et al. 2013; Popescu et al. 2016; Pappalardo et al. 2018; Crawford et al. 2018), material properties (Jager et al. 2013; Fikos et al. 2014; Panek et al. 2014; Kaczmarek et al. 2015; Mita et al. 2018; Claudio et al. 2018), probable slip surface identification (Drahor et al. 2006; Yilmaz 2007; Jomard et al. 2010; Souisa et al. 2015; Ardi and Mimin 2016; Ling et al. 2016; Asriza et al. 2017; Kaminski and Zientara 2017) and identification of ground water table (Lapenna et al. 2005; Heincke et al. 2010; Bièvre et al. 2012; Akpan et al. 2015; Crawford 2018; Khalil et al. 2018; Hazreek et al. 2018). Table 1 shows the summary of such previous works on ERT applications for different aspects of landslide investigation specifically.

Keeping these in view, the present case study is aimed to integrate both the borehole investigation information and interpretation of electrical resistivity tomography (ERT) results using Wenner array for subsurface characterization of Pakhi Landslide in terms of material thickness/layering and identification of probable slip surface.

**Table 1** Review on application of ERT in landslide investigation

Sl. no.	Aspects of landslide investigation	Results	References
1	Slip surface location	Slip surface is identified as the contact between layers of soil or rock that is impermeable to the mass of soil on top of it	Drahor et al. (2006); Yilmaz, (2007); Jomard et al. (2010); Souisa et al. (2015); Ling et al. (2016); Ardi and Mimin (2016); Asriza et al. (2017); Kaminski and Zientara (2017)
2	Material thickness/layering	ERT has the capability of giving information both on the lithostratigraphic sequences and the geometry of the landslide body (lateral extension and thickness). It helps to determine the vertical delineation of the sliding volume which supposed to have different physical parameters than that of the non-sliding material	Reci et al. (2013); Popescu et al. (2016); Crawford et al. (2018); Pappalardo et al. (2018)
3	Evaluation of material properties	ERT has helped in material characterization as one of the major factors responsible for slope failure since different soil and rock materials possess different resistivity value	Jager et al. (2013); Kaczmarek et al. (2015); Panek et al. (2014); Fikos et al. (2014); Claudio et al. (2018); Mita et al. (2018)
4	Identification of water saturated zone	The mechanism of landslides through higher groundwater levels often occur in residual soil slopes and colluvial deposits. The presence of a relatively less impervious layer causes the water caught in it and form a water saturated zone resulting in slope failure	Lapenna et al. (2005); Heincke et al. (2010); Jomard et al. (2010); Bièvre et al. (2012); Akpan et al. (2015); Crawford (2018); Hazreek et al. (2018); Khalil et al. (2018)

Pakhi landslide: the study area

Pakhi landslide is one of the major active landslides along Rishikesh–Badrinath National Highway (NH-58) which has high importance for both strategic and tourism activities in Uttarakhand State of India. The landslide falls within the latitude 30.464°N to 30.467°N and longitude 79.457°E to 79.460°E (Fig. 1). The slide is about 1.8 km away from Pakhi village and at about a distance of 9 km ahead of Pipalkoti on Rishikesh–Badrinath National Highway (NH-58) corridor of Garhwal Himalayas in Uttarakhand. This landslide falls within Pipalkoti window of Tejam group (Heim and Gansser 1939) which is made up of predominantly dolomites of Deoban formation (Validiya 1980) with various degrees of weathering as a

result of extreme climatic condition within the region. For the study area falling under Uttarakhand hydro-meteorological division of India, the long period annual average rainfall is 1580.9 mm. The mean rainfall of 1229.1 mm during monsoon period (June–September) contributes 77.7% of annual rainfall (1580.9 mm). Contribution of pre-monsoon (March–May) rainfall and post-monsoon (October–December) rainfall in annual rainfall is of the order of 9.9 and 5.7%, respectively. The monthly average rainfall for monsoon period during June to September is 167.8, 428.1, 426.3 and 206.9 mm, respectively. The mean minimum and maximum temperatures during monsoon period vary from 14.8 to 16.9 °C and 22.9 to 25.9 °C, respectively. The pre-monsoon mean minimum and maximum temperatures vary from 6.6 to 13.9 °C and 17.6 to 24.6 °C, respectively. The post-monsoon mean minimum

Fig. 1 **a** Topographic map of Pakhi landslide showing locations of boreholes, ERT profile lines and lithological cross section lines; **b** panoramic view of Pakhi landslide indicating the ERT profile lines
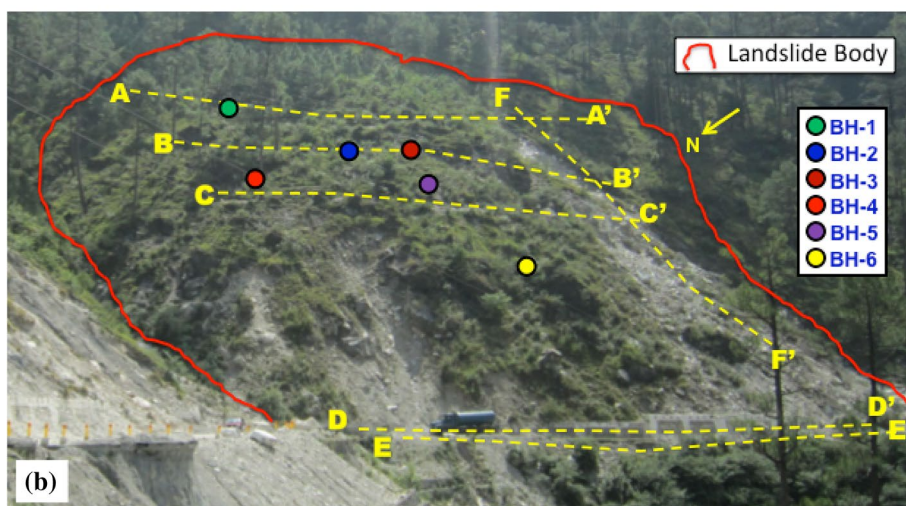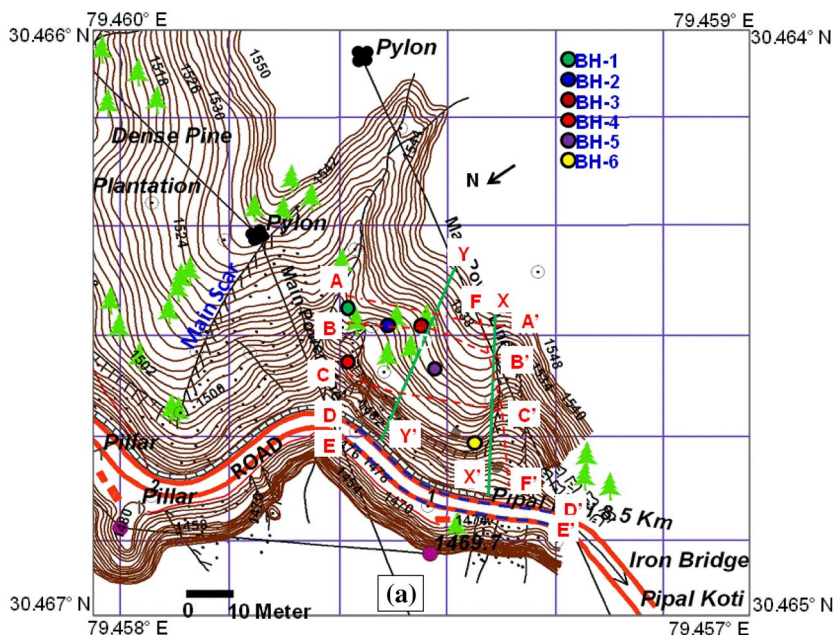
and maximum temperatures vary from 3.8 to 10.5 °C and 13.6 to 20.6 °C, respectively.

The main body of the landslide is defined by its extension on both the flanks and from crown to toe based on field observations. This landslide is bounded by two natural streams on both left and right flanks. These streams join the Alaknanda River downhill. The crown of the landslide is defined by the main scar beyond which on uphill side there is no sign of distress and tension cracks and also there is a break in slope between crown and the uphill steep slope with exposure of dolomitic rocks. The stable portion beyond the crown of the landslide has also been reported in the previous work on ground-based monitoring of this landslide area (Kanungo et al. 2017). The toe of the landslide exists at the road (NH-58) level. The landslide body is marked on the field photograph of the landslide (Fig. 1b).The topographic map with elevation contours on 1:1000 scale with 2 m contour interval of the landslide area (Fig. 1a) has been prepared. The elevation at the toe of the landslide (at road level) is 1476 m and that at the crown of the landslide is 1526 m above msl.

The landslide is basically a retrogressive debris slide with shallow overburden material resting on a steep slope (Kanungo et al. 2013). The general slope angle of the landslide amounts to 55°–60° with a direction of N320°. The base rock in the slide area is dolomitic limestone. The unfavourable discontinuity (bedding plane) has a dip of about 45°–55° with a dip direction of N320° (almost as that of slope). It has a dip–slope relationship with respect to the slope direction which makes this discontinuity plane favourable for sliding of overburden material (colluvium and weathered dolomites) along this plane. The landslide has the main scar on the uphill slope and a number of minor (secondary) scars developed along the radial transverse tension cracks all over the landslide body. There is a clear indication of detachment and displacement of the order of sub-metre to a metre along all these tension cracks, which indicates the retrogressive nature of sliding activity (Kanungo et al. 2013). The landslide is spread over a length of 112 m in total at the road level with two active stretches on left and right flanks having spread lengths of about 57 m and 15 m, respectively. Initially, the debris slide along a narrow channel on the left flank and at the excavated height at road level was initiated due to the road widening process. During the monsoon period (rainy season), this region witnesses frequent occurrence and reactivation of landslides due to increase in the amount of water infiltration into the colluvial soils on the slopes, thereby reducing the shear strength properties of the soil. Due to heavy precipitation in this area during the monsoon season (specifically August to September of 2010), this active portion of the slide got extended towards its right side and is also progressing retrogressively towards uphill side.

In previous study on this particular landslide (Kanungo et al. 2013), it has been reported based on the field observation on landslide scar faces that there exists three different layers of material such as top soil (colluvium), weathered dolomites and fresh dolomites across depths. Based on the disturbed sampling and laboratory geotechnical analysis of colluvium material, it is further reported that the colluvium contains about 62–65% of gravel and sand and 35–38% of silt and clay content with a specific gravity of 2.67. Further, the cohesion under unsaturated condition is of the order of 0.2 kg/cm^2 with friction angle of about 36°–42°. Under saturated condition, the colluvium is almost cohesionless and the friction angle varies in the range of 34°–40°.

Methodology

In this study, the surface and subsurface characteristics of the landslide were investigated using an integrated approach. The previous work (Kanungo et al. 2013) as described in "Pakhi Landslide: the study area" has also helped in executing and analysing the present work in a better way. The subsurface mapping in this present case has been carried out using borehole investigation and ERT survey techniques to compliment each other in accurately delineating the interfaces of different material layers across depth and also identifying the probable slip surfaces in the landslide area. The borehole locations and the profile lines for ERT survey are shown on the contour map and the field photograph of the landslide area (Fig. 1).

The outline of the methodology for subsurface characterisation of the landslide is given in the flow chart (Fig. 2). Geophysical investigation using ERT and geotechnical investigation using borehole drilling and logging (Strelec et al. 2017; Bellanova et al. 2018) methods were carried out in this landslide area during pre-monsoon period (May 2018). The previous field mapping and published literatures, GPS point data and Google Earth Image helped in locating the borehole points and also the ERT profile lines. Under geotechnical investigation of the landside, six boreholes were made (BH 1–6) out of which one is located at the crown portion of the landslide (BH 1), three are located in the middle portion (BH 2, 3 and 4) and rest two are located above road level at the toe portion (BH 5 and 6) of the landslide body. The drilling has been carried out using rotary drilling method with double tube core barrels. The drilled materials were carefully logged and recovered samples were labelled and kept in the core boxes. Under geophysical investigation of the landslide, ERT survey along six profile lines were performed out of which three profiles are located across the landslide slope along different elevation contours
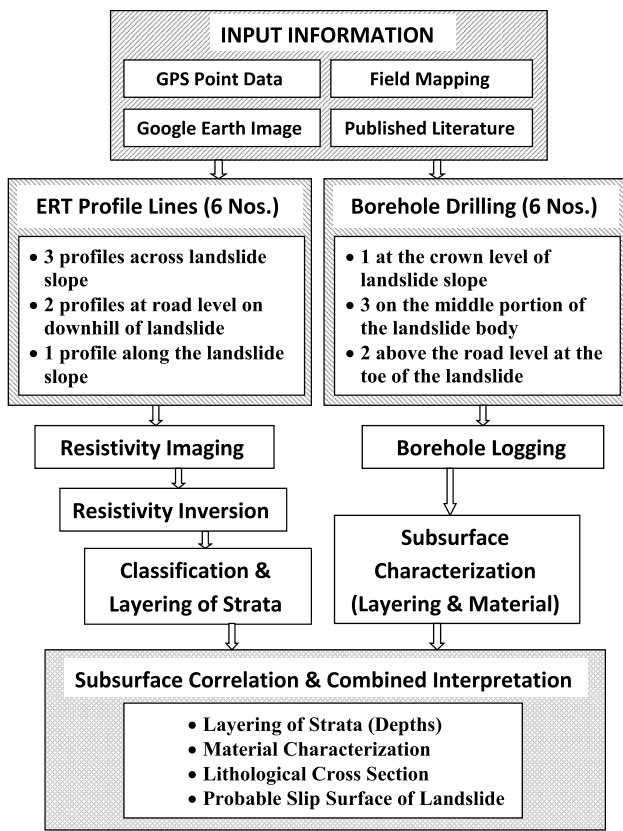
INPUT INFORMATION
- GPS Point Data
- Field Mapping
- Google Earth Image
- Published Literature

ERT Profile Lines (6 Nos.)
- 3 profiles across landslide slope
- 2 profiles at road level on downhill of landslide
- 1 profile along the landslide slope

Borehole Drilling (6 Nos.)
- 1 at the crown level of landslide slope
- 3 on the middle portion of the landslide body
- 2 above the road level at the toe of the landslide

Resistivity Imaging

Borehole Logging

Resistivity Inversion

Classification & Layering of Strata

Subsurface Characterization (Layering & Material)

Subsurface Correlation & Combined Interpretation
- Layering of Strata (Depths)
- Material Characterization
- Lithological Cross Section
- Probable Slip Surface of Landslide

Fig. 2 Methodology flow chart for subsurface characterization of the landslide (Drahor et al. 2006; Yilmaz 2007; Jomard et al. 2010; Jager et al. 2013; Reci et al. 2013; Fikos et al. 2014; Panek et al. 2014; Kaczmarek et al. 2015; Souisa et al. 2015; Ardi and Mimin 2016; Ling et al. 2016; Popescu et al. 2016; Asriza et al. 2017; Kaminski and Zientara 2017; Claudio et al. 2018; Crawford et al. 2018; Mita et al. 2018; Pappalardo et al. 2018)
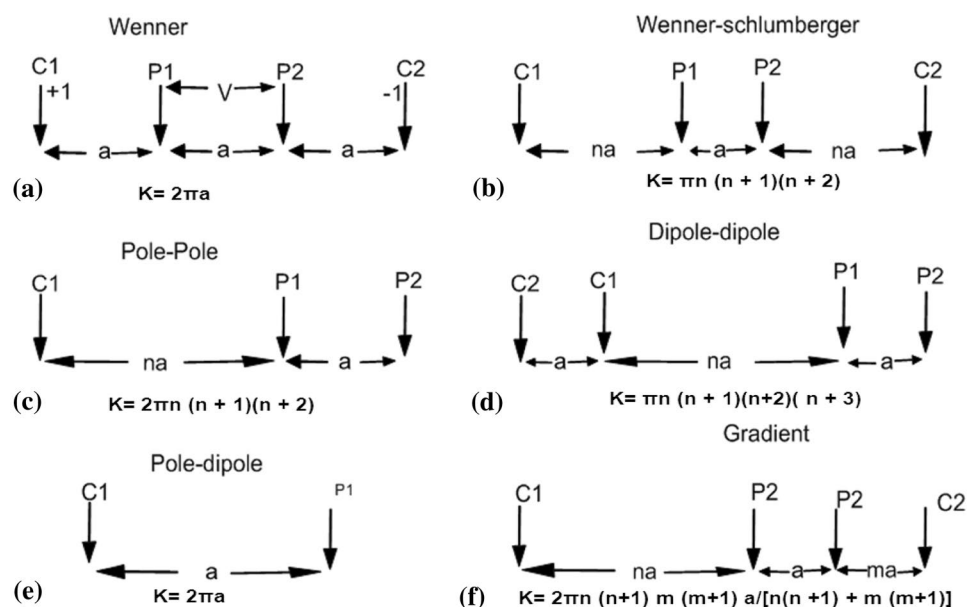
(AA′, BB′ and CC′), two profiles are located at the road level in the toe portion (DD′ and EE′) of the landslide and rest one profile is located along the slope on the left flank (FF′) of the landslide body. The borehole investigation data in association with the ERT inverse images were interpreted to reveal the landslide characteristics in terms of lithologies/materials and their interfacial depth and to delineate the probable slip surfaces as carried out by many researchers (Drahor et al. 2006; Yilmaz 2007; Göktürkler et al. 2008; Jomard et al. 2010; Reci et al. 2013; Giocoli et al. 2015; Souisa et al. 2015; Ardi and Mimin 2016; Fressard et al. 2016; Ling et al. 2016; Popescu et al. 2016; Zhang 2016; Asriza et al. 2017; Kaminski and Zientara 2017; Uhlemann et al. 2017; Bellanova et al. 2018).

Electrical resistivity tomography (ERT)

The application of ERT method in landslide investigation has helped in providing information about electrical resistivity distribution of the subsurface materials. The resistivity contrast between different types of earth materials is a reasonable means to identify different material characteristics, which has been attributed to the degree of weathering, moisture content and mineralogical composition of such earth material.

The field procedure comprises current multi-electrode system, which is connected at a fixed distance according to the specification of electrode configuration (Schlumberger, Wenner, Wenner-Schlumberger, Dipole–Dipole, etc.) on the ground. The current (I) is injected into the subsoil through the electrode and the voltage (V) is measured. The values of V and I depend on the geometric factor of the array

Fig. 3 Commonly used ERT array and their geometric factors (Loke et al. 2013)

(a) Wenner $K = 2\pi a$

(b) Wenner-schlumberger $K = \pi n (n + 1)(n + 2)$

(c) Pole-Pole $K = 2\pi n (n + 1)(n + 2)$

(d) Dipole-dipole $K = \pi n (n + 1)(n+2)(n + 3)$

(e) Pole-dipole $K = 2\pi a$

(f) Gradient $K = 2\pi n (n+1) m (m+1) a/[n(n +1) + m (m+1)]$

configuration as indicated in Fig. 3. Accordingly, the resistivity can be estimated using Eq. (1):

$$\rho = k\frac{\Delta V}{I}, \tag{1}$$

where ρ is the resistivity, k is the geometric factor, I is the current flow and ΔV is the potential difference.

The electrical resistivity tomography is usually derived from the inversion of the apparent resistivity (Perrone et al. 2014). One of the famous inversion algorithms is RES-2Dinv (Loke and Barker 1996; Loke et al. 2003) which is based on a smoothness-constrained least-squares method. It allows to obtain two-dimensional sections through finite differences or finite elements computations. The root mean square error (RMS) can be used to evaluate the fit of the resistivity model obtained which gives percentage difference between the measured and calculated values.

This ERT-based method was adopted for this research work to delineate the internal strata, to define the geometric features as well as to estimate the thickness of the sliding materials within the landslide body. This method has widely been used by many researchers in recent times to investigate various forms of landslide and Table 1 shows the summary of such previous works on landslide investigation specifically.

Technically, various arrays can be used in obtaining the ERT information depending on the subsoil depth of investigation, sensitivity to vertical and horizontal changes, strength of signal and horizontal data coverage (Loke 1999; Naudet et al. 2008). The advantages and limitations of different ERT arrays used in landslide study and reported by various researchers over the time are listed in Table 2. In this study, a multi-cable electrode imaging system, ABEM terameter, was used for the acquisition of data. The equipment comprises 48 electrodes, which provide accurate imaging at the depth of investigation within the sliding body. Wenner array, which is robust, high signal-to-noise ratio and high characterisation of horizontal discontinuities (as listed in Table 2) and used and reported by many researchers for landslide investigation (Sumanovac 2006; Lee et al. 2008; Sass et al. 2008; Shan et al. 2013; Khalil et al. 2018; Pappalardo et al. 2018), was used for the acquisition of data with different electrode spacings depending on the stretch available on the landslide slope. The inversion of the data obtained from the field was carried out using RES2Dinv software developed by Loke and Barker (1996). The electrical resistivity data were acquired along six profiles, out of which five profiles are transverse to the landslide slope direction along the elevation contours and one profile is in the longitudinal direction of the landslide slope across the elevation contours (Fig. 1). The different parameter details such as length of profiles, electrode spacings, number of electrodes and type of array used in different ERT profile lines are given in Table 3.

Borehole drilling

Six boreholes were drilled within the landslide body to unveil the subsurface lithology and probable slip surface of the landslide. This information will further compliment the results obtained from the ERT survey. The locations of the boreholes are shown in Fig. 1. The drilling operation has been carried out using rotary drilling with double tube core drilling method instead of triple tube with wire line drilling method due to some constraints. The drilling method used may cause some mechanical breakage and thereby loss of soil and softer materials in the core recovery process. The depths of the boreholes vary from place to place depending on the drilling conditions and the depth of the in situ rock strata. The borehole 1 (BH-1) which is at a higher elevation and almost at the crown of the landslide was drilled up to 18 m depth. Three boreholes (BH-2, 3 and 4) at the middle portion of the landslide body were drilled up to 21 m, 22 m and 19 m depths, respectively. Two boreholes (BH-5 and 6) at further lower elevations on landslide slope just above the road level were drilled up to 16.5 m depths each. The samples recovered from the boreholes were properly logged to decipher the nature and depth of material encountered at different depths.

Results and discussion

Subsurface characterisation of the landslide using borehole logging

Based on the borehole logging information, it is observed that two to three layers of materials/lithologies are encountered in different boreholes along the depths vertically down (Table 4 and Fig. 4a). BH-1 is located within the upper crown part of the landslide slope about 2 m away from profile A–A′ (Fig. 1). The data from the borehole indicate a top layer of colluvium deposits up to 9.0 m which is followed by weathered dolomites up to 13.5 m and then by fresh dolomite rock up to the drilling depth (i.e., 18.0 m). BH-2 and 3 were drilled along profile B–B′ about 15 m apart. BH-2 encounters colluvium up to 1.5 m, colluvium and boulders from 1.5 to 6.0 m, weathered dolomites from 6.0 to 18.0 m and fresh dolomites from 18.0 to 21.0 m as interpreted from the core recovery. The logs from BH-3 show that the colluvium, weathered dolomites, fresh dolomites and again weathered dolomites are present (Fig. 4a) with interfaces between these layers at 1.5 m, 6.0 m and 10.5 m, respectively, and it could not be drilled beyond 22 m to encounter fresh dolomitic bed rock again beyond weathered dolomites

Table 2 Advantages and limitations of different ERT array used in landslide study

S. no.	Array (references)	Advantages	Limitations
1	Wenner-Schlumberger: (Zhang, 2016; Fressard et al. 2016; Bellanova et al. 2018; Rezaei et al. 2018, Mita et al. 2018; Szokoli et al. 2018)	Sensitivity to changes in both horizontal and vertical directions It has higher signal-to noise ratio than other configurations Good for shallow and non-complex landslide	It obtains narrower data than dipole–dipole array
2	Dipole–Dipole: (Jardani et al. 2012; Reynolds 2011; Crawford et al. 2018; Mita et al. 2018; Crawford et al. 2018)	High sensitivity to horizontal changes in resistivity Determination of isometric structures Good for Deep seated and Complex landslide	Insensitive to vertical changes in the resistivity More prone to errors because of very small signal strength
3	Wenner: (Sumanovac, 2006; Sass et al. 2008; Lee et al. 2008; Shan et al. 2013; Khalil et al. 2018; Pappalardo et al. 2018)	Robust; high signal-to noise ratio Characterization of horizontal discontinuities Good for shallow and non-complex landslide	Poor in determination of vertical resolution Susceptible to near-surface, lateral variations in resistivity which can be misinterpreted in terms of depth variations in resistivity
4	Schlumberger: (Panek et al. 2014; Prodán et al. 2015; Hazreek et al. 2018)	Gives good mapping for the vertical change of the resistivity	Very sensitive voltmeters are required Limited to simple, horizontally layered structures
5	Pole–Dipole: (Jomard et al. 2007; Grandjean et al. 2011)	To increase the depth of investigation, it has relatively good horizontal coverage Higher signal strength compared to dipole–dipole array Lower sensitivity to telluric noise when compared with pole–pole array	Lower signal strength when compared with Wenner and Wenner-Schlumberger arrays
6	Pole-Pole: (Chang et al. 2012; Zerathe and Lebourg 2012)	Widest horizontal coverage Deepest depth of investigation	Prone to large amount of telluric noise which can affect the quality of measurements Poorest resolution

Table 3 Parameters of the ERT survey for data acquisition

Profile lines / Parameters of ERT array	A–A′	B–B′	C–C′	D–D′	E–E′	F–F′
Length of profile (m)	94	72	72	94	94	94
Electrode spacing (m)	2	1.5	1.5	2	2	2
Number of electrodes	48	48	48	48	48	48
Type of array	Wenner	Wenner	Wenner	Wenner	Wenner	Wenner

Table 4 Borehole logging results of the boreholes drilled on the landslide slope

Location	Lithology	Depth (m) From	To
BH-1	Colluviums	0	9.0
	Weathered dolomites	9.0	13.5
	Fresh dolomites	13.5	18.0
BH-2	Colluviums	0	1.5
	Colluviums and boulders	1.5	6.0
	Weathered dolomites	6.0	18
	Fresh dolomites	18	21
BH-3	Colluviums	0	1.5
	Weathered dolomites	1.5	6.0
	Fresh dolomites	6.0	10.5
	Weathered dolomites	10.5	22
BH-4	Colluviums	0	1.5
	Weathered dolomites	1.5	8.5
	Fresh dolomites	8.5	19
BH-5	Weathered dolomites	0	7.5
	Fresh dolomites	7.5	16.5
BH-6	Weathered dolomites	0	10.5
	Fresh dolomites	10.5	16.5

due to site and operational constraints. BH-4, drilled up to 19.0 m, encountered three layers such as colluvium, weathered dolomites and fresh dolomites with interfaces at depths of 1.5 m and 8.5 m, respectively. The drilling core samples collected from BH-4 are shown in Fig. 4b as an example. BH-5 and 6, drilled up to 16.5 m each, encountered two strata layers such as weathered dolomites and fresh dolomites with interfaces at depths of 7.5 m and 10.5 m. respectively (Fig. 4a). In all these six boreholes, no water table was encountered up to the drilling depths. Further, geotechnical laboratory analysis of collected drilling core samples could not be performed and included in this research work.

Subsurface characterisation of the landslide using ERT survey

The electrical resistivity of any material is usually controlled by different factors such as water content, porosity, clay content, etc. Generally, there are wide ranges in electrical resistivity values for any particular type of material and, accordingly, electrical resistivity values cannot be directly interpreted in terms of lithology/materials. Keeping these in view, the results were interpreted with the help of literatures, exploratory boreholes, and direct resistivity measurements to calibrate the ERT and to correlate electrical resistivity values with the lithological characteristics (Chang et al. 2011; Crawford 2018). It is to be noted here that the electrodes during the ERT survey were put into the sloping ground vertically down and 2D ERT images are created on the plane perpendicular to the sloping surface. Therefore, all the resistivity interpretations made in the present study depict the depths perpendicular to the sloping surface of the landslide.

It is observed from the ERT images of all the profile lines (Fig. 5) that with a profile length of 94 m the depth of penetration perpendicular to the sloping surface is around 17–17.5 m (for profiles AA′, DD′, EE′ and FF′) and with a profile length of 72 m the depth of penetration perpendicular to the sloping surface is about 12.9 m (for profiles BB′ and CC′) as tabulated in Table 5. The results obtained from electrical resistivity imaging indicate a wide range of resistivity values. This may be due to the variation in the subsurface characteristics of the material of the landslide body (Chang et al. 2011). As interpreted from the resistivity values, there exists mainly three-layered strata in the landslide body (Table 5 and Fig. 5). This is also in agreement with the previous study on the particular landslide as mentioned in "Pakhi Landslide: the study area" (Kanungo et al. 2013). The first layer (I) has an assumed lower resistivity range of < 1000 Ωm, which can be interpreted as colluvium as observed in borehole logs. The second layer (II) is observed to have a somehow middle range of resistivity values of the order of 1000–4500 Ωm and can be inferred as weathered dolomites (as observed in borehole logs). The third layer (III), which can be interpreted as fresh dolomitic limestone as per borehole logs, has still a higher range of resistivity values > 4500 Ωm. The slip surface of the landslide was observed to be the intersection layer between the colluviums and the weathered dolomites (Crawford et al. 2018). Apart from the low clay contents (Kanungo et al. 2013), the higher resistivity values can also be observed as a result of less water infiltration into the landslide body as the ERT measurements have been

Fig. 4 a The drill core logs of the six boreholes (BH-1 to BH-6) and **b** the drilling cores of BH-4

(a)
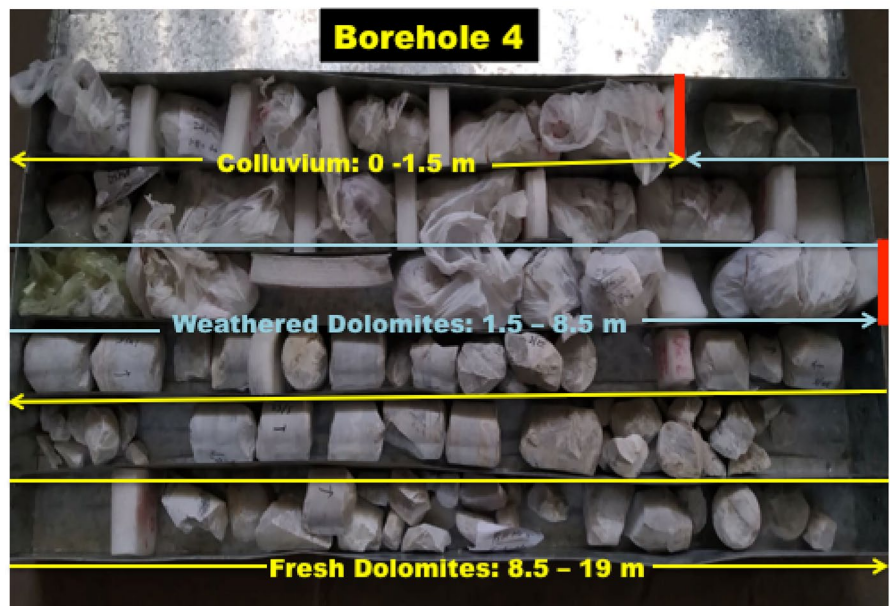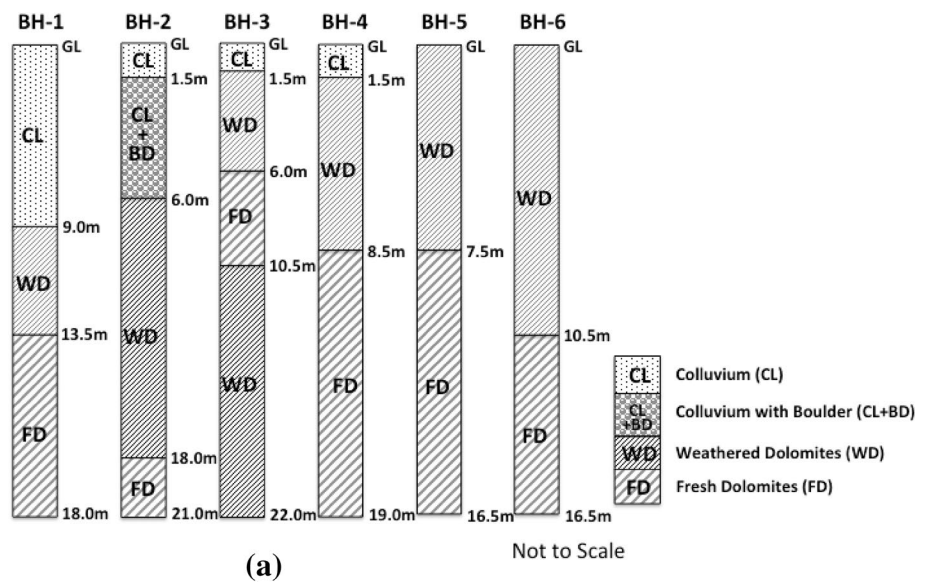
(b)

carried out during pre-monsoon period indicating no water-saturated zones and no water table was encountered during the drilling operation also.

Interpretation of ERT profile line A–A′

The inverse model resistivity section of A–A′ profile line (Fig. 5a) is interpreted and it is observed that at central section of profile (47 m on the surface) the colluvium (layer I) with low resistivity ($< 1000\ \Omega m$) is encountered up to a depth of about 10 m; this colluvium layer extends on the left flank of the landslide at a similar depth up to 66 m of the profile line horizontally on the surface and

extends on the right flank of the landslide with an increasing depth up to about 13.5 m at 34 m of the profile line on the surface. At the central resistivity section beyond 10 m depth, the second layer (layer II) of weathered dolomitic limestone is encountered till the total depth of penetration (i.e., 17.2 m). The interface between the colluvium and weathered dolomite layers is interpreted as the slip surface of the landslide. This is also supported by the evidence from previous study (Kanungo et al. 2013) as the bedding plane of dolomites is in dip–slope relationship with the slope and the overlying colluvium slides down on the bedding plane of the underlying weathered dolomitic rocks. Such interpretations are also made by many researchers
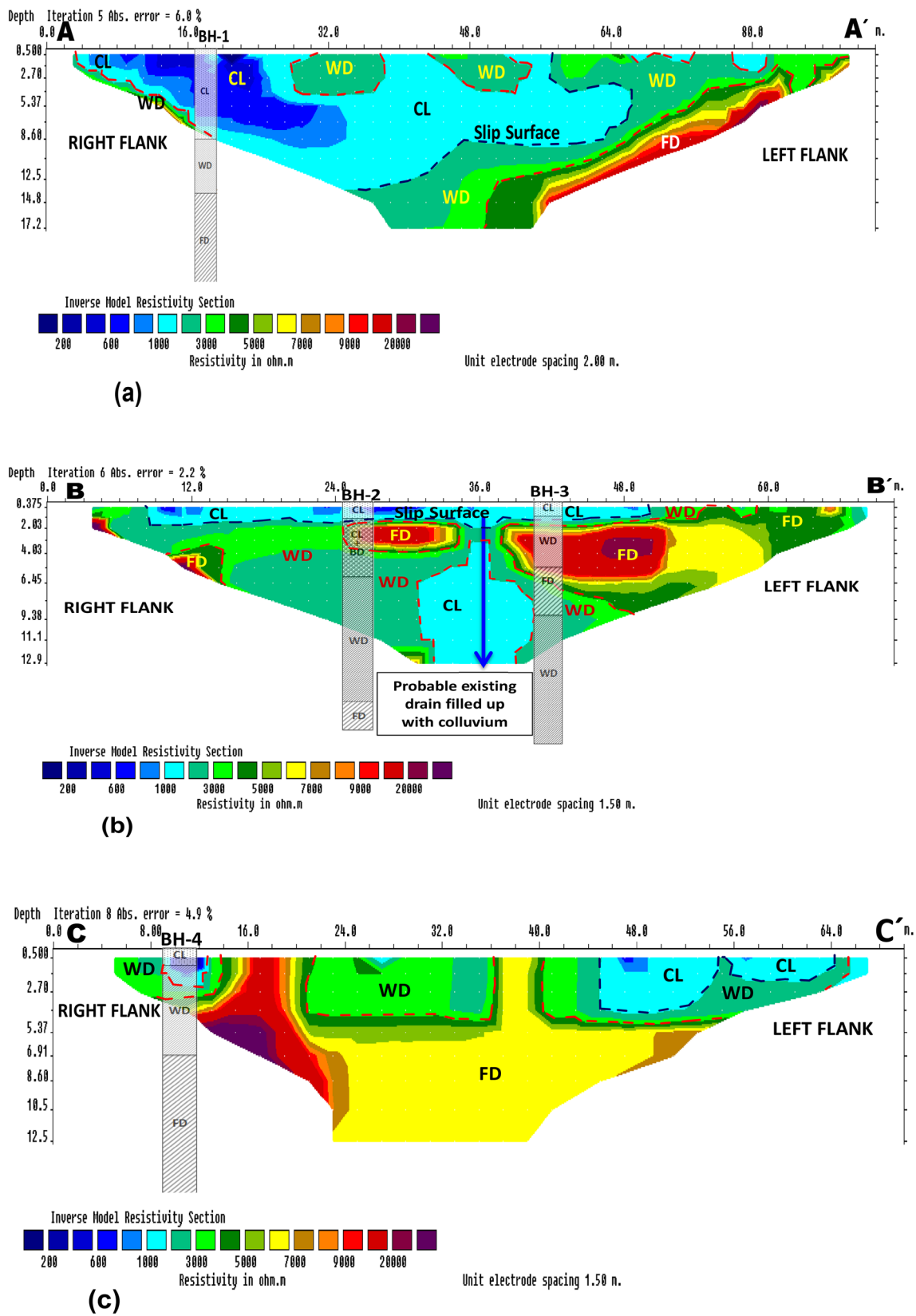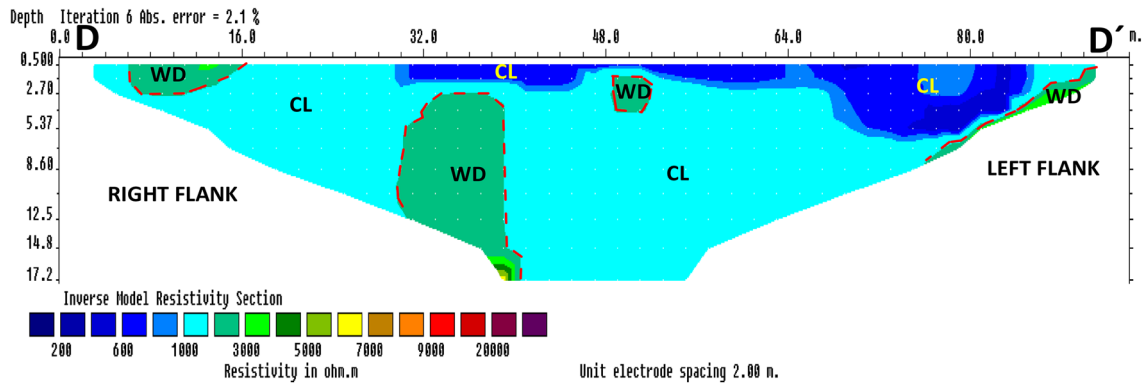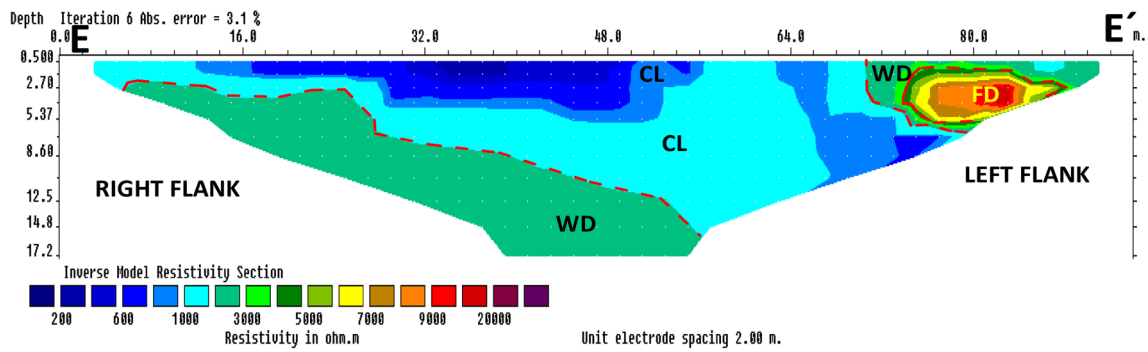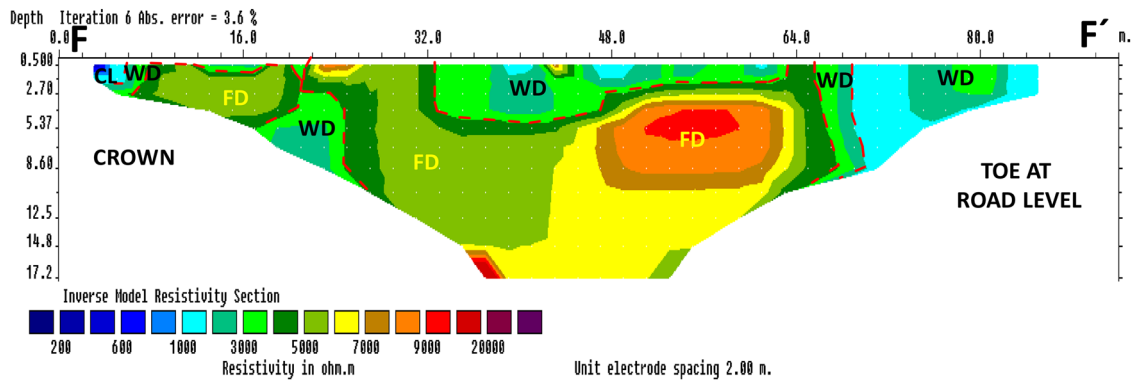
(a)

(b)

(c)

Fig. 5 Inverse model of resistivity sections along profile lines: **a** A–A′, **b** B–B′, **c** C–C′, **d** D–D′, **e** E–E′ and **f** F–F′ (*CL* colluvium, *WD* weathered dolomites, *FD* fresh dolomites, *BD* boulder, *BH* borehole)
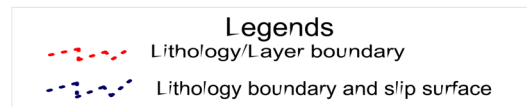
(d)

(e)

(f)

Fig. 5 (continued)

Table 5 Result of electrical resistivity tomography [I = 1st layer (colluviums), II = 2nd layer (weathered dolomites), III = 3rd layer (fresh dolomites)]

Profile lines	Total depth of penetration (m)	Layers	Resistivity (Ωm)	Lithology
A–A′	17.2	I	<1000	Colluviums (CL)
		II	1000–4500	Weathered dolomites (WD)
		III	>4500	Fresh dolomites (FD)
B–B′	12.9	I	<1000	Colluviums (CL)
		II	1000–4500	Weathered dolomites(WD)
		III	>4500	Fresh dolomites(FD)
		–	>4500	Boulder of fresh dolomites (BD)
C–C′	12.9	II	1000–4500	Weathered dolomites(WD)
		III	>4500	Fresh dolomites (FD)
D–D′	17.2	I	<1000	Colluviums (CL)
		II	1000–4500	Weathered dolomites (WD)
E–E′	17.5	I	<1000	Colluviums (CL)
		II	1000–4500	Weathered dolomites(WD)
		III	>4500	Fresh dolomites(FD)
F–F′	17.2	I	1000–4000	Weathered dolomites (WD)
		III	>4500	Fresh dolomites (FD)

based on ERT and other investigations (Drahor et al. 2006; Jomard et al. 2010; Souisa et al. 2015; Ling et al. 2016; Ardi and Mimin 2016; Asriza et al. 2017; Kaminski and Zientara 2017).

Further, on the left flank of the landslide, the interface between second (weathered dolomite) and third (fresh dolomite) layers is encountered at a depth of 13.5 m at 51 m of the profile line on the surface; the depth of this interface decreases beyond this point and tapers at a depth of about 2.5 m at 84 m of the profile line on the surface. On the surface at right flank of the landslide, the colluvium layer is encountered with stray patches of weathered dolomites and at left flank of the landslide; weathered dolomites are encountered beyond 57 m of the profile line.

Interpretation of ERT profile line B–B′

In the inverse model of resistivity section of B–B′ profile line of 72 m stretch (Fig. 5b), it is observed on the surface that the weathered dolomites are encountered up to 8 m followed by colluvium up to 51 m beyond which again weathered dolomites are witnessed up to 55 m followed by fresh dolomites up to 72 m (end of the scan length). On the right flank of the landslide across depth, the colluvium layer extends up to about 2 m beyond which weathered dolomites are encountered. Also, an existence of a boulder of somewhat fresh dolomite at a depth of 2–4 m just beneath the colluvium layer at around 25–34 m along profile line can be interpreted on the right flank. On the left flank of the landslide area at 42 m on surface scan line across depth, the colluvium layer also extends up to about

2 m followed by a thin layer of weathered dolomites of about 0.5 m up to 2.5 m depth beyond which fresh dolomites are encountered up to a depth of 6.5 m followed by the weathered dolomitic layer again. On the left flank, the fresh dolomitic layer at a depth of 2.5 m extends from 37.5 to 55 m along the profile line and then appears on the surface from 55 to 72 m. Across depth this fresh dolomite layer extends gradually from 3 m depth at 37.5 m on surface up to 9 m depth at 48 m on surface. This indicates that this layer is unaffected by the weathering process. The colluvium at central section of the scan line (at 36 m on surface) extends all across the depth of interpretation (i.e., 12.9 m depth) and achieves a width of 9.5 m (from 31 to 40.5 m on surface) at a depth of 6.5 m onwards. This overall inverse model of resistivity section gives an impression of an existing natural drain at the central portion of this profile line on the landslide slope which has been buried with time by slided colluviums (refer to Fig. 5b).

Interpretation of ERT Profile Line C–C′

Along the profile line of the inverse model of the resistivity section of C–C′ (Fig. 5c) on the surface, weathered dolomitic strata has been encountered up to 14 m initially with colluvium from 9 to 12.5 m, at 21.5–36.0 m and 39–45 m up to a depth of almost 4.0–4.5 m uniformly. Beyond the weathered dolomitic layer, fresh dolomitic bed rock is encountered all around up to a maximum interpretable depth of 12.5 m along with two surface exposures at 14.0–21.5 m and 36–39 m along profile

line. On surface from 45 m till the end of scan line, the colluvium layer is encountered initially up to a depth of 4 m and tapering up to a depth of 2 m at the end of the scan line.

Interpretation of ERT profile line D–D′

It could be observed from the inverse model of the resistivity section of D–D′ profile line (Fig. 5d) along the hill side road section of the landslide slope that on the surface all along the profile line colluvium layer is encountered except from 6 m up to 16 m where weathered dolomites are encountered up to an average depth of 3 m. All across the scanned depth also the colluvium layer is interpreted except few encounters of weathered dolomites such as from 30 to 40 m on surface beyond 2.5 m depth up to the scanned depth (i.e., 17.2 m) and a small patch from 48 to 52 m on surface at a depth from 1 m up to 4 m. The appearance of a thick deposit of colluvium almost all along the profile line of 94 m on road side is in agreement with the observed fact that this is the depositional area at the toe of the active landslide (Kanungo et al. 2013) where thick deposit of debris/colluvium can be expected.

Interpretation of ERT profile line E–E′

It is interpreted from the inverse model of the resistivity section of E–E′ profile line (Fig. 5e) on the valley side road section of the landslide slope that on the surface along the profile line colluvium layer is encountered from the beginning up to 70 m with an initial average depth of 2–3 m up to 26 m on surface and then with a gradually increasing depth up to maximum 17.2 m (equivalent to scanned depth) up to 56 m on surface along the profile line. Beyond this colluvium layer, weathered dolomite layer is encountered. Beyond 70 m on the surface along the profile line, weathered dolomites of around 1–2 m thickness are underlain by fresh dolomites. This interpretation of thick colluvial deposits reiterating such interpretation in case of ERT profile line D–D′ (refer to "Interpretation of ERT Profile Line D–D′") can again be inferred as the depositional area at the toe of the active landslide (Kanungo et al. 2013) where thick deposit of debris/colluvium can be expected. Further, these interpretations can give an idea about the width of the depositional fan of the order of about 90 m on hill side and 70 m on valley side (as the weathered and fresh dolomite exposures may have restricted the deposition beyond 70 m) at the road level.

Interpretation of ERT profile line F–F′

It may be interpreted from the inverse model of the resistivity section of F–F′ profile line (Fig. 5f) along the landslide slope across the contours on the left flank of the landslide

that from the top along the slope up to initial 6 m colluvium is encountered; 6–8 m weathered dolomites; 8–32 m almost fresh dolomites with a very thin cover of weathered dolomites at places; 32–63 m again weathered dolomites; 63–66 m fresh dolomites; 66–69 m weathered dolomites; 69–74 m colluvium; 74–82 m weathered dolomites; and then from 82 m up to the end of the scan line again colluvium layers are encountered. Across the depth perpendicular to the sloping surface, the weathered dolomites from 32 to 63 m on surface are underlain by fresh dolomites beyond a depth of 5 m initially and beyond 1.5 m in the later part. Just above the road level, there is a mixed signature of colluvium and weathered dolomites from 68 m till the end of the profile line across the depth of the ERT interpretation at the toe of the landslide. This interpretation from ERT is also in agreement with the visual observation from the site and further supports the findings from ERT profile lines D–D′ and E–E′ (refer to "Interpretation of ERT Profile Line D–D′" and "Interpretation of ERT Profile Line E–E′" and Fig. 5d, e) on depositional area at the toe of the active landslide (Kanungo et al. 2013).

Correlation of the results and combined interpretation

It is to be noted here that the boreholes were made on the landslide sloping surface vertically down and the borehole logs were interpreted accordingly. However, the electrodes for the ERT survey were put into the landslide sloping surface vertically down and 2D ERT images are created on the plane perpendicular to the sloping surface. Therefore, all the resistivity interpretations made in the present study depict the depths perpendicular to the sloping surface of the landslide, whereas the borehole logs depict the depths vertically down the ground surface. Still to obtain a comparative visualisation, depth wise information from ERT and borehole log on different planes is put together (Fig. 5a–c).

If the borehole log of BH-1 is superimposed on the ERT profile of A–A′ (Fig. 5a) at about 18 m along the profile line, it is revealed that the interface between colluvium and weathered dolomite layers at 9 m depth are almost matching. Beyond 9 m depth, the information from ERT image is unavailable. So, it could not be correlated with the borehole log. However, the extrapolation of the interface between colluvium and weathered dolomite layers can be correlated with that of borehole log (Fig. 5a).

When the log of BH-2 is superimposed on the ERT profile of B–B′ (Fig. 5b) at about 25 m along the profile line, it can be observed that the top colluvium layer is almost existing in both borehole log and ERT section up to a depth of 1.5 m. Beyond 1.5 m depth, BH-2 log displays colluvium along with boulders of dolomites up to 6 m whereas the ERT section B–B′ reveals initial thin layer of weathered dolomite

and then boulder of fresh dolomite up to about 4 m. Beyond 6 m depth along the borehole, again a matching of weathered dolomite layer is observed both from ERT and borehole interpretations. Though there is a mismatch between borehole interpretation (colluvium with boulders) and ERT interpretation (weathered dolomites with boulders), it can be interpreted in this case as colluvium with boulders because of the fact that borehole information is more authentic in comparison to ERT result and the colluvial material can be produced from the weathered dolomites. This mismatch in depth interpretation of material layer may also be attributed to the ERT and borehole log information on different planes with respect to the sloping ground.

As the log of BH-3 is cross correlated with the ERT profile of B–B′ (Fig. 5b) at about 42 m along the profile line, it can be observed that the top colluvium layer is matching in both the subsurface sections. However, the subsequent layer across depth from 1.5 to 6 m is interpreted as initial thin layer of weathered dolomites followed by fresh dolomites in ERT image, whereas it is observed as weathered dolomites in drilling cores. Similarly, the subsequent material from 6 to 10.5 m depths is interpreted as initial thin layer of fresh dolomites followed by weathered dolomites in ERT image, whereas it is observed as fresh dolomites in drilling cores. Beyond a depth of 10.5 m, weathered dolomites are interpreted by both ERT and borehole methods. Hence, there is a mismatch in the weathering status of material from 1.5 to 10.5 m depth though the parent rock dolomite could be interpreted from ERT results and ascertained with the drilling cores. Therefore, the limitation in interpretation of the weathering status of the rock strata from ERT inverse image may be looked into with further research on this aspect. This also can be resolved with both pre- and post-monsoon ERT results for identifying the water-saturated zones vis-à-vis borehole results as investigated by many researchers (Lapenna et al. 2005; Heincke et al. 2010; Jomard et al. 2010; Bièvre et al. 2012; Akpan et al. 2015; Crawford 2018; Hazreek et al. 2018; Khalil et al. 2018) instead of only pre-monsoon data as done in this present case study. Also, this mismatch in depth interpretation of material layer may also be attributed to the ERT and borehole log information on different planes with respect to the sloping ground. Further, adoption of a better drilling technique of wireline triple tube rotary drilling over a double tube rotary drilling method for such exploratory investigation may ascertain better core recovery without mechanical breakage and core losses in the drilling process and thereby can address such mismatch and doubts on the strata.

As the core log of BH-4 is superimposed on the ERT profile section of C–C′ (Fig. 5c) at about 10 m along the profile line, it can be correlated that in both the sections the sequence of appearance of all the three layers (colluvium, weathered dolomites and fresh dolomites) is same. There is

a perfect match in the interface of colluvium and weathered dolomite layers in both the results. Also, the extrapolation of fresh dolomites as interpreted in ERT image down the depth will match with the fresh dolomites obtained from the drilling cores beyond 8.5 m depth. However, there may be a mismatch in the interface between weathered and fresh dolomite layers across depth. Though the parent rock dolomite could be interpreted from both the investigation results, the possible reason and further research on such aspects have already been discussed in the previous paragraph.

The core log information of BH-5 and 6 could not be correlated with any of the ERT profile sections as these locations do not coincide.

From the above information and correlation, it could be stated that the types of materials/lithologies, subsurface interfaces between different material layers, probable slip surface and the depositional area at the toe of the landslide could be revealed in a successful manner to a great extent based on the integration of various information obtained from previous work on the particular landslide (Kanungo et al. 2013), related works by other researchers (Drahor et al. 2006; Yilmaz 2007; Jomard et al. 2010; Heincke et al. 2010; Jager et al. 2013; Reci et al. 2013; Fikos et al. 2014; Panek et al. 2014; Giocoli et al. 2015; Kaczmarek et al. 2015; Souisa et al. 2015; Ardi and Mimin 2016; Ling et al. 2016; Popescu et al. 2016; Zhang 2016; Asriza et al. 2017; Kaminski and Zientara 2017; Strelec et al. 2017; Rezaei et al. 2018; Crawford et al. 2018; Claudio et al. 2018; Bellanova et al. 2018; Pappalardo et al. 2018; Mita et al. 2018) and present investigations through boreholes and ERT surveys. This also helped in overcoming the shortcoming of localised information at places of surface exposures of all the material layers based only on physical mapping (Kanungo et al. 2013; Strelec et al. 2017).

ERT based landslide model

Two lithological cross sections were drawn along profiles X–X′ and Y–Y′ (as marked in Fig. 1) on the left and right flanks of the landslide body, respectively, based on the interpretations from the inversion models of different ERT sections (Fig. 6).

The X–X′ cross section is intersected by the ERT profiles A–A′, B–B′ and C–C′ at 80 m, 61 m and 64 m on the ERT scan lines, respectively, and at an elevation of about 1537 m, 1519 m and 1500 m, respectively. On the X–X′ cross section at the intersection of ERT profile A–A′, colluvium layer up to 2.5 m depth, weathered dolomite layer up to another 1.5 m depth and fresh dolomites beyond the weathered dolomite layer were observed on the plane perpendicular to the sloping surface of the landslide. At the intersection of X–X′ cross section and ERT profile B–B′, a thin layer with 0.5 m depth of weathered dolomites is
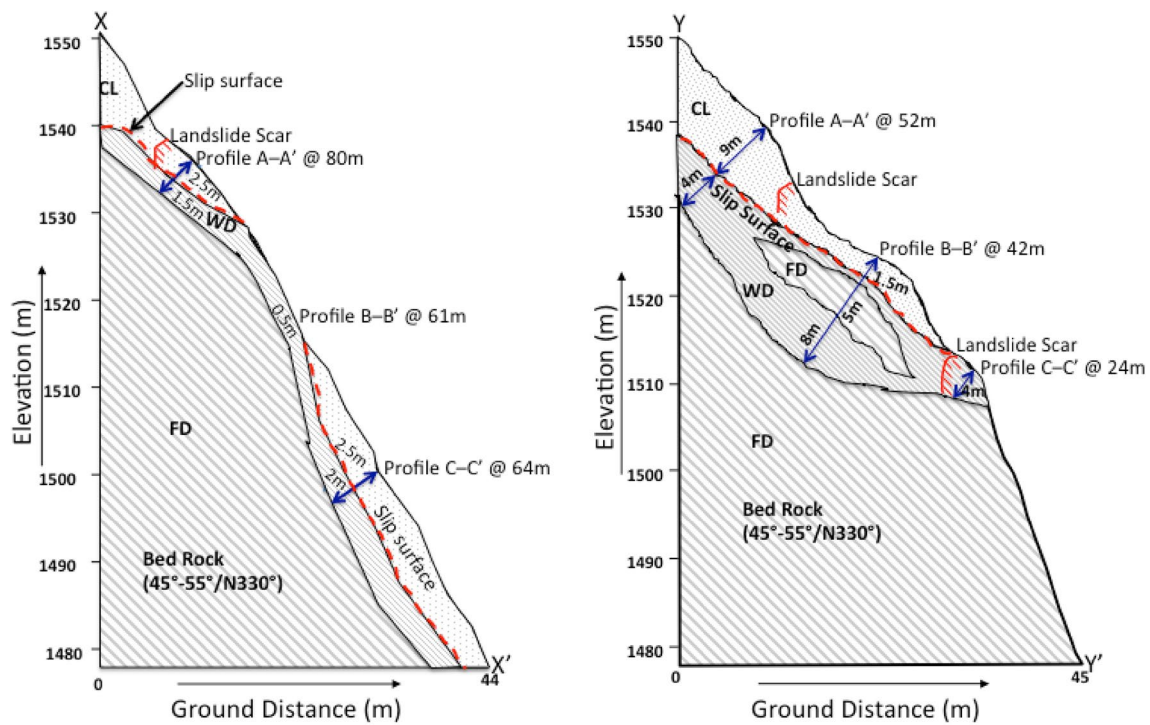
Fig. 6 Lithological cross sections along X–X′ and Y–Y′ (as shown in Fig. 1) drawn from ERT inversion sections (*CL* colluvium, *WD* weathered dolomites, *FD* fresh dolomites)

underlain by fresh dolomites. At the intersection of X–X′ cross section and ERT profile C–C′, colluvium layer up to 2.5 m depth, weathered dolomite layer up to another 2 m depth and fresh dolomites beyond the weathered dolomites layer were observed on the plane perpendicular to the sloping surface of the landslide. Combining these information, a depth wise material model along X–X′ profile section on the left flank of the landslide could be established (Fig. 6). It could be observed from this model that colluvium layers of about 2.5 m thick are existing at the crown of the landslide from EL 1550 m up to EL 1530 m and above the road level (NH-58) from EL 1515 m up to EL 1478 m demarcating the slip surface from the underlying weathered dolomites.

The Y–Y′ cross section is intersected by the ERT profiles A–A′, B–B′ and C–C′ at 52 m, 42 m and 24 m on the ERT scan lines, respectively, and at an elevation of about 1540 m, 1525 m and 1512 m, respectively. At the intersection of Y–Y′ cross section and ERT profile A–A′, colluvium layer up to 9 m depth, weathered dolomite layer up to another 4 m depth and fresh dolomites beyond the weathered dolomites layer were observed on the plane perpendicular to the sloping surface of the landslide. On this cross section at the intersection of ERT profile B–B′, sequentially 1.5 m depth of colluvium, a thin layer with 0.5 m depth of weathered dolomites, 5 m depth of fresh dolomites, 8 m depth of weathered dolomites again and fresh dolomites beyond weathered dolomites were observed. Further at the

intersection of Y–Y′ cross section and ERT profile C–C′, a weathered dolomite layer of 4 m thick was observed to be underlain by fresh dolomites. A depth wise material model along Y–Y′ profile section on the right flank of the landslide could be established (Fig. 6) by combining these information. From this model, a thick colluvium layer of about 9 m thick at the crown and reducing gradually to a thickness of about 1–1.5 m up to EL 1515 m could be observed which demarcates the slip surface from the underlying weathered dolomites of about 4–13.5 m thick.

It can be observed from both the X–X′ and Y–Y′ profile models that the crown portion of the landslide on the right flank (refer to Y–Y′ profile) has comparatively a greater volume of colluvium deposit with respect to the left flank (refer to X–X′ profile). Therefore, the crown portion of the right flank is more vulnerable to sliding phenomenon and that of the left flank is more prone to erosion. It can also be inferred that during coming monsoon season with the sliding/erosion of these overlying colluvium deposits the rain water may further percolate into the underlying weathered and fresh dolomites along the bedding planes to further deteriorate the strength properties of these strata. Therefore, the sliding phenomena will proceed to deeper levels and in a retrogressive manner during monsoon seasons if adequate mitigative measures are not implemented to protect the current sliding process.

Conclusions

The present work with an integrated approach for subsurface investigation is the first such attempt in one of the landslides in Indian Himalayas and has been adopted using the information obtained from six boreholes drilled on the landslide and six sections of ERT profiling across and along the landslide from crown to the toe. This work has also been strengthened by the research contributions on ERT application for landslide investigation by various researchers. The results reveal the reliability of ERT and borehole methods in a complimentary manner in determining the depths and types of different material/lithology layers, probable slip surface and the extent of depositional fan at the toe of the landslide area. It is observed that the ERT profiling could delineate these features of the landslide in a continuous manner; thereby overcoming the limitations of localised information through borehole investigation and physical mapping of surface exposures on cut-slope faces.

The disagreement in depth of material/strata in ERT and borehole information shown on the same plane could be due to their actual interpretations on different planes with respect to the sloping surface of the landslide. The disagreement in depth of interface between fresh and weathered strata in ERT and borehole information could reveal the limitation in interpretation of the weathering status of the rock strata using ERT technique. This aspect can be looked into with further research on interpretation of both pre- and post-monsoon ERT images of the same profile lines for identifying the water-saturated zones as investigated by many researchers in the subject area. The present case study has a limitation of using only pre-monsoon data and thereby could not delineate any water-saturated zone across the depth. No water table was also encountered during the drilling process.

Visualising the parallel ERT profile lines in sequence from crown to the toe (i.e., AA′–EE′) of the landslide, it can be observed that at the crown portion there is a huge cover of colluvium (of the order of 9–12.5 m thick) at the central and left flank of the landslide (AA′ profile). Moving down the landslide slope, in the middle part (BB′ profile) of the landslide a thin cover of colluvium of the order of 1.5–2 m is interpreted along with a huge deposit of colluvium at the central portion probably along an existing drain. Further down the slope (CC′ profile line) no colluvium cover is observed in the central and right flank area except on left flank area of the order of 2.5–4 m thickness. At and around the toe of the landslide (DD′ and EE′ profile lines), there is a huge accumulation of colluvial material due to sliding in the past above which the road has been built. Based on these interpretations, it can be stated that sliding has already occurred from the lower portion of the landslide area exposing the weathered and fresh dolomitic rocks which is also

evident from the on-site field observations. However, there is a huge cover of colluvium at the crown of the landslide and to some extent in the middle part of the landslide which will slide down in a retrogressive manner. Therefore, based on all the interpretation made in the present case study, previous work on this particular landslide (Kanungo et al. 2013) and contributions in the related aspects from various researchers, it can be inferred that the Pakhi landslide is a retrogressive landslide of translational debris slide in nature where the slip surface exists at the interface of colluvial layer and weathered dolomitic layer having a dip-slope relationship.

Further, based on the landslide model drawn from the ERT interpretations, it can be stated that the crown portion of the right flank is more vulnerable to sliding phenomenon and that of the left flank is more prone to erosion. It can also be inferred that during coming monsoon seasons with the sliding/erosion of the overlying colluvium deposits the sliding phenomena will proceed to deeper levels and in a retrogressive manner with the aggravated weathering process due to rain water seepage.

Therefore, such non-invasive geophysical ERT technique for landslide investigation can be effective in association with other investigation techniques for delineating the depth and type of the landslide materials, geometry of the landslide across depth, slip surface and extent of depositional area, etc. Such techniques will be quite useful in reducing the number of boreholes for subsurface characterisation; thereby reducing the cost of the investigation and also with minimum disturbance to the already unstable hill slope through drilling. However, minimum drilling operation is essential to properly interpret the depth and type of actual material appearance in a complementary manner.

References

Akpan AE, Abidemi OI, Nse UE (2015) Geophysical investigation of Obot Ekpo landslide site, Cross River State, Nigeria. J Afr Earth Sci 109:154–167

Ardi ND, Mimin IM (2016) Sliding zone identification of landslide area using resistivity method in Cijambe, Subang West Java. AIP Conf Proc 1708:070001. https://doi.org/10.1063/1.4941174

Asriza S, Kristyanto THW, Indra TL, Syahputra R, Tempessy AS (2017) Determination of the landslide slip surface using electrical resistivity tomography (ERT) technique. 4th World Landslide Forum, Ljubljana, Slovenia (Europe). In: Mikoš M, Arbanas Z, Yin Y, Sassa K (eds) Advancing culture of living with landslides, vol. 2: advances in landslide technology. Springer, Berlin,

pp 53–60. https://doi.org/10.1007/978-3-319-53487-9 (ISBN 978-3-319-53486-2)

Bellanova J, Giuseppe G, Giocoli A, Luongo R, Perron A, Lapenna V, Piscitelli S (2018) Electrical resistivity tomography surveys for the geoelectric characterization of the Montaguto landslide (southern Italy). Eng Geol 234:272–281

Bièvre G, Jongmans D, Winiarski T, Zumbo V (2012) Application of geophysical measurements for assessing the role of fissures in water infiltration within a clay landslide (Trieves area, French Alps). Hydrol Process 26:2128–2142

Chang KT, Lin ML, Dong JJ, Chien CH (2011) The Hungtsaiping landslides: from ancient to recent. Landslides 9(2):205–214

Chang P, Chen C, Chang S, Wang T-B, Wang C-Y, Hsu S-K (2012) An investigation into debris flow induced by Typhoon Morakot in the Siaolin Area, Southern Taiwan, using electrical resistivity imaging method. Geophys J Int 188:1012–1024

Claudio V, Matthew E, Jan B, Lukáš Ž, Mirko F, John SC (2018) Investigation of landslide failure mechanisms adjacent to lignite mining operations in North Bohemia (Czech Republic) through a limit equilibrium/finite element modelling approach. Geomorphology 5:44. https://doi.org/10.1016/j.geomorph.2018.08.006

Crawford MM (2018) Hydrologic monitoring and 2-D electrical resistivity imaging for joint geophysical and geotechnical characterization of shallow colluvial landslides (2018). Theses and Dissertations–Earth and Environmental Sciences, p 61

Crawford MM, Bryson LS, Woolery EW, Wang Z (2018) Using 2-D electrical resistivity imaging for joint geophysical and geotechnical characterization of shallow landslides. J Appl Geophys 157:37–46

Cruden DMA (1991) A simple definition of a landslide. Bull Eng Geol Environ 43:27–29

de Bari C, Lapenna V, Perrone A, Puglisi C, Sdao F (2011) Digital photogrammetric analysis and electrical resistivity tomography for investigating the Picerno landslide (Basilicata region, southern Italy). Geomorphology 133(1):34–46

Drahor MG, Gokturkler G, Berge MA, Kurtulmus TO (2006) Application of electrical resistivity tomography technique for investigation of landslides: a case from Turkey. Environ Geol 50:147–155

Fikos I, Vargemezis G, Papageorgiou F (2014) Landslide investigation with the use of electrical resistivity tomography: a case study in Epirus Greece. http://www.unibuc.ro/facultati/geologiegeofizica/docs/2014/noi/20_13_09_02P20_GO2014.pdf. Accessed 9 July 2017

Fressard MA, Maquaire O, Thiery Y, Davidsona R, Lissak C (2016) Multimethod characterisation of an active landslide: case study in the Pays d'Auge plateau (Normandy, France). Geomorphology 270:22–39

Giocoli A, Stabile T, Adurno I, Perrone A, Gallipoli M, Gueguen E, Norelli E, Pistitelli S (2015) Geological and geophysical characterization of the South-Eastern side of the high Agri valley (Southern Apennines Italy). Nat Hazards Earth Syst Sci 15:315–323

Göktürkler G, Balkaya C, Erhan Z (2008) Geophysical investigation of a landslide: the Altındağlandslide site, İzmir (western Turkey). J Appl Geophys 65:84–96

Grandjean G, Courry JC, Sanchez O, Bitri A, Garambois S (2011) Structural study of the Ballanz landslide (French Alps) using geophysical imagery. J Appl Geophys 75:537–542. https://doi.org/10.1016/j.jappgeo.2011.07.008

Grandjeans G, Malet JP, Bitri A, Méric O (2007) Geophysical data fusion by fuzzy logic for imaging the mechanical behaviour of mudslides. Bull Soc Géol Fr 178:127–136

Hazreek ZAM, Nizam ZM, Aziman M, Dan MFMd, Shaylinda MZN, Faizal TBM, Aishah MAN, Ambak K, Rosli S, Rais Y, Ashraf MIM, Alel MNA (2018) Mapping on slope seepage problem using electrical resistivity imaging (ERI). J Phys Conf Ser 995(2018):012091. https://doi.org/10.1088/1742-6596/995/1/012091

Heim A, Gansser A (1939) Central Himalaya Geological observations of Swiss. Hindustan Publishing Corporation (India), Delhi

Heincke B, Gunther T, Dalsegg E, Ronning JS, Ganerod GV, Elvebakk H (2010) Combined three-dimensional electrical and seismic tomography study on the Akens rockslide in Western Norway. J Appl Geophys 70:292–306

Jager D, Sandmeier C, Schwindt D, Terhorst B (2013) Geomorphological and geophysical analyses in a landslide area near Ebermannstadt, Northern Bavaria. E&G Quat Sci J 62(2):150–161. https://doi.org/10.3285/eg.62.2.06

Jardani A, Revil A, Dupont JP (2012) Stochastic joint inversion of hydrogeophysical data for salt tracer test monitoring and hydraulic conductivity imaging. Adv Water Resour. https://doi.org/10.1016/j.advwatres.2012.08.005

Jomard H, Lebourg T, Guglielmi Y, Tric E (2010) Electrical imaging of sliding geometry and fluids associated with a deep seated landslide (La Clapière, France). Earth Surf Process Landf 35:588–599

Jomard H, Lebourg T, Tric E (2007) Identification of the gravitational boundary in weathered gneiss by geophysical survey: La Clapière landslide (France). J Appl Geophys 62:47–57

Jongmans D, Garambois S (2007) Geophysical investigation of landslides: a review. Bull Soc Géol Fr 178(2):101–112

Kaczmarek Ł, Mieszkowski R, Kopaczyński M, Pacanowski G (2015) Application of electrical resistivity tomography (ERT) in the investigation of quaternary land slide zones, based on the selected regions of Płock slope. Stud Quat 31(2):101–107. https://doi.org/10.2478/squa-2014-0010

Kamiński M, Zientara P (2017) Geophysical model and displacement of active landslide—an example from Jastrzębia Góra Cliff (Northern Poland). In: Mikoš M et al (eds) Advancing culture of living with landslides, vol 3. Springer, Berlin, pp 341–348

Kanungo DP, Pain A, Sharma S (2013) Stability assessment of a potential debris slide in Garhwal Himalayas, India. Indian Landslides 6(2):9–20

Kanungo DP, Maletha AK, Singh M, Sharma N (2017) Ground based wireless instrumentation and real time monitoring of Pakhi Landslide, Garhwal Himalayas, Uttarakhand (India). In: Mikoš M et al (eds) Advancing culture of living with landslides, vol 3. Springer, Berlin, pp 293–300. https://doi.org/10.1007/978-3-319-53487-9

Khalil MA, Bobst A, Mosolf J (2018) Utilizing 2D electrical resistivity tomography and very low frequency electromagnetics to investigate the hydrogeology of natural cold springs near Virginia City, Southwest Montana. Pure Appl Geophys 175:3525–3538

Lapenna V, Lorenzo P, Perrone A, Piscitelli S, Rizzo E, Sdao F (2005) 2D electrical resistivity imaging of some complex landslides in Lucanian Apennine chain, southern Italy. Geophysics 70:B11–B18

Lee C, Yang H, Liu H, Wen L, Wang Z, Chen J (2008) A study of the hydrogeological environment of the Lishan landslide area using resistivity image profiling and borehole data. Eng Geol 98:115–125

Ling C, Xu Q, Ran J, Lv H (2016) Application of electrical resistivity tomography for investigating the internal structure of a Translational landslide and characterizing its groundwater circulation (Kualingzi landslide), South China. J Appl Geophys 131:154–162

Lissak C, Maquaire O, Malet J-P, Bitri A, Samyn K, Grandjean G, Bourdeau C, Reiffsteck P, Davidson R (2014) Airborne and ground-based data sources for characterizing the morpho-structure of a coastal landslide. Geomorphology 217:140–151

Loke MH (1999) Electrical imaging surveys for environmental and engineering studies: a practical guide to 2-D and 3-D surveys. http://www.abem.se/files/res/2Dnotes.pdf. Accessed June 6 2017

Loke MH, Barker RD (1996) Rapid least-squares inversion of apparent resistivity pseudosections by a quasi-Newton method. Geophys Prospect 44(1):131–152

Loke MH, Acworth I, Dahlin T (2003) A comparison of smooth and blocky inversion methods in 2-D electrical imaging surveys. Explor Geophys 34:182–187

Loke MH, Chambers JE, Rucker DF, Kuras O, Wilkson PB (2013) Recent development in the direct current geoelectrical imaging method. J Appl Geophys 95:135–156

Malet J-P, Maquaire O, Calais E (2002) Le GPS en géomorphologie dynamique. Application à la surveillance de mouvements de terrain (super-Sauze, Alpes du Sud, France)/GPS in geomorphological studies. Application to the survey of landslides (super-Sauze, South France). Géomorphol Relief Process Environ 8:165–179

Mita M, Glazer M, Kaczmarzyk R, Dąbrowski M, Mita K (2018) Case study of electrical resistivity tomography measurements used in landslides investigation, Southern Poland. Contemp Trends Geosci 7(1):110–126. https://doi.org/10.2478/ctg-2018-0007

Naudet V, Lazzari M, Perrone A, Loperte A, Piscitelli S, Lapenna V (2008) Integrated geophysical and geomorphological approach to investigate the snowmelt–triggered landslide of Bosco Piccolo village (Basilicata, southern Italy). Eng Geol 98(3–4):156–167

NDMA (2009) Management of landslides and snow avalanches, 2009. Government of India, New Delhi, p 144

Panek T, Hradecky J, Silhan K (2014) Application of electrical resistivity tomography (ERT) in the study of various types of slope deformations in anisotropic bedrock: case studies from Flysch Carpathians. Stud Geomorphol Carpatho Balc 42:7–73

Pappalardo G, Imposa IS, Barbano IMS, Grassi IS, Mineo IS (2018) Study of landslides at the archaeological site of Abakainon necropolis (NE Sicily) by geomorphological and geophysical investigations. Landslides 15:1279–1297

Perrone A, Piscitelli S, Vincenzo L (2014) Electrical resistivity tomography technique for landslide investigation: a review. Berichte Geol B Appl Landslide Monit 135:65–82 **(ISSN 1017-8880)**

Popescu M, Serban R, Urdea P, Onaca AL (2016) Conventional geophysical surveys for landslide investigations: two case studies from Romania. Carpathian J Earth Environ Sci 11(1):281–292

Prodán TH, Prácser E, Balogh J, Kis É, Klébesz R (2015) Geoelectric tomography carried out on a mass movement site of Kulcs Settlement (in Hungary). J Geogr Nat Disaster 5:149. https://doi.org/10.4172/2167-0587.1000149

Reci H, Muceku Y, Jata I (2013) The use of ERT for investigation of Berzhita landslide, Tirana Area, Albania, landslides and monitoring. Springer, Berlin, pp 117–123

Reynolds JM (2011) An introduction to applied and environmental geophysics. Wiley-Blackwell, Hoboken, NJ

Rezaei S, Shooshpasha I, Rezaei H (2018) Empirical correlation between geotechnical and geophysical parameters in a landslide zone (case study: nargeschal Landslide). Earth Sci Res J 22(3):195–204

Sass O, Bell R, Glade T (2008) Comparison of GPR, 2D-resistivity and traditional techniques for the subsurface exploration of the Öschingen landslide, Swabian Alb (Germany). Geomorphology 93:89–103

Sastry R, Mondal S (2013) Geophysical characterization of the Salna Sinking zone, Garhwal Himalaya, India. Surv Geophys 34:89–119

Shan W, Hu Z, Jiang H, Guo Y, Wang C (2013) Mechanism of permafrost landslide based on GPS and Resistivity Surveying. In: Wang F, Miyajima M, Li T, Shan W, Fathani T (eds) Progress of geo-disaster mitigation technology in Asia. Environmental Science and Engineering (Environmental Engineering). Springer, Berlin, Heidelberg, pp 349–361. https://doi.org/10.1007/978-3-642-29107-4_18

Souisa M, Hendrajaya L, Handayani G (2015) Determination of landslide slip surface using geoelectrical resistivity method at Ambon City Moluccas-Indonesia. Int J Emerg Technol Adv Eng 5(7), www.ijetae.com **(ISSN 2250-2459, ISO 9001:2008)**

Strelec S, Mesec J, Graba K, Jug J (2017) Implementation of in situ and geophysical investigation methods (ERT and MASW) with the purpose to determine 2D profile of landslide. Acta Montan Slovaca 22(4):345–358

Sumanovac F (2006) Mapping of thin sandy aquifers by using high resolution reflection seismics and 2-D electrical tomography. J Appl Geophys 58:144–157

Szokoli K, Szarka L, Metwaly M, Kalmar J, Pracser E, Szalai S (2018) Characterization of a landslide by its fracture system using electric resistivity tomography and pressure probe methods. Acta Geod Geophys 53:15–30. https://doi.org/10.1007/s40328-017-0199-3

Travelletti J, Malet JP (2012) Characterization of 3D geometry of flow-like landslide: a methodology based on the integration of heterogeneous multi-source data. Eng Geol 128:30–48

Uhlemann S, Chambers J, Wilkinson P, Maurer H, Merritt A, Meldrum P, Kuras O, Gunn D, Smith A, Dijkstra T (2017) Four-dimensional imaging of moisture dynamics during landslide reactivation. J Geophys Res Earth Surf 122:398–418

Validiya KS (1980) Geology of Kumaun Lesser Himalaya. Wadia Institute of Himalayan Geology, Dehradun

van Westen C, Ghosh S, Jaiswal P, Martha T, Kuriakose S (2013) From landslide inventories to landslide risk assessment; an attempt to support methodological development in India. In: Margottini C, Canuti P, Sassa K (eds) Landslide science and practice. Springer, Berlin Heidelberg, pp 3–20

Yilmaz S (2007) Investigation of Gu¨rbulak landslide using 2D electrical resistivity image profiling method (Trabzon, Northeastern Turkey). J Environ Eng Geophys 12(2):199–205

Zerathe S, Lebourg T (2012) Evolution stages of large deep-seated landslides at the front of a subalpine meridional chain (Maritime-Alps, France). Geomorphology 138:390–403

Zhang X (2016) Numerical simulation study on the detection of weak structural plane of rock slope by using 3D electrical resistivity tomography. Engineering 8:438–444. https://doi.org/10.4236/eng.2016.870.41